JOURNAL OF APPLIED ELECTROCHEMISTRY **16** (1986) 544–554

Electrochemistry of the chalcocite–xanthate system

C. S. O'DELL, G. W. WALKER, P. E. RICHARDSON

US Department of the Interior, Bureau of Mines, Avondale Research Center, 4900 LaSalle Road, Avondale, MD 20782–3393, USA

Received 18 April 1985; revised 22 July 1985

The interactions between chalcocite and ethylxanthate have been examined in an electrochemical–microflotation cell containing a particle-bed working electrode. Cyclic voltammetry has shown the formation of a chemisorbed product commencing at -0.5 V versus SCE with a bulk oxidation product, possibly cuprous xanthate, forming above -0.23 V. Relating the charge passed on a potentiostated mineral bed after addition of xanthate to spectrophotometric changes in xanthate concentration suggested the presence of a fast chemical reaction and a charge transfer reaction. The strong correlation between flotation response and potential indicates that chemisorption of ethylxanthate produces a layer sufficiently hydrophobic for chalcocite flotation.

1. Introduction

Previous studies [1–5] have suggested that the adsorption of xanthate collector onto sulphide minerals occurs primarily through electrochemical interactions. Flotation and collector–mineral interactions have been shown to be strongly dependent on electrode potential; however, the exact reaction mechanisms remain unclear.

Recent work [6] with chalcocite (Cu_2S) identified a potential range of -0.5 to 0 V versus the saturated calomel electrode (SCE) where three distinct processes involving xanthate ions were observed to occur in chalcocite–xanthate–oxygen systems. The postulated reactions were as follows:

1. A reaction of xanthate with Cu(II)species

$$\mathrm{Cu(II)} + 2\mathrm{X}^- = \mathrm{CuX_2} \qquad (1a)$$

where Cu(II) is produced by the open-circuit dissolution of chalcocite

$$\mathrm{Cu_2S} = \mathrm{Cu_{2-\lambda}S} + \lambda\mathrm{Cu(II)} + 2\lambda e \qquad (1b)$$

2. A substitution reaction

$$\mathrm{Cu(OH)_2} + 2\mathrm{X}^- = \mathrm{CuX_2} + 2\mathrm{OH}^- \qquad (2a)$$

where the oxidation product $Cu(OH)_2$ is produced by a corrosion reaction

$$\mathrm{Cu_2S} + 2\lambda\mathrm{OH}^- = \mathrm{Cu_{2-\lambda}S} + \lambda\mathrm{Cu(OH)_2} + 2\lambda e \qquad (2b)$$

3. An oxidation reaction

$$\mathrm{Cu_2S} + \lambda\mathrm{X}^- = \mathrm{Cu_{2-\lambda}S} + \lambda\mathrm{CuX} + \lambda e \qquad (3)$$

which is assumed to occur at a bare (unoxidized) chalcocite surface.

Examination of these reactions reveals that the two most significant parameters by which their relative rates may be controlled are dissolved oxygen concentration and electrochemical potential. At open circuit, reduction of dissolved oxygen provides the conjugate cathodic reaction for Reactions 1b, 2b and 3. The rate of oxygen reduction, as well as the rates of Reactions 1b, 2b and 3, is likewise dependent on electrochemical potential. Since Reactions 1b and 2b are precursors of reactions 1a and 2a, each of the reaction involving xanthate (reactions 1–3) are dependent on dissolved oxygen and electrochemical potential.

The anodic and cathodic processes are assumed to be independent of each other with the overall reaction rate determined by the net balance between the cathodic and anodic currents. In flotation circuits, the injection of air into the pulp provides a dissolved oxygen level. The mixed potential is thus fixed by the oxygen reduction reaction and chalcocite oxidation reaction. Removal of the dissolved oxygen eliminates the dominant cathodic reduction and permits examination of the anodic processes by applied potential techniques.

0021–891X/86 $03.00 + .12

For the present work, the system was enclosed in a glove box in an attempt to obtain negligible oxygen levels. Advantage was taken of the large ratio of surface area to solution volume to study xanthate adsorption on the particle bed electrode using conventional flow-through ultraviolet (UV) spectrophotometry. Studies are reported on (1) the cyclic voltammetric characteristics of chalcocite bed electrodes in the absence and presence of xanthate, (2) the electrolysis charge associated with the reaction between xanthate and chalcocite, and (3) associated changes in xanthate concentration measured spectrophotometrically.

2. Experimental procedure

The microflotation–electrochemical cell, flow system and equipment have been described previously [7]. Fig. 1 shows the modified system enclosed in a controlled nitrogen atmosphere dry box maintained at a pressure of 12 mm of water. The system was constructed with a Pyrex glass cell, Teflon tubing and a Teflon pump*. Ultrahigh purity nitrogen, used to purge the dry box and the solution, was passed over hot copper filings to remove trace oxygen. All experiments were conducted in a 0.05 M buffered sodium tetraborate solution (pH 9.2) purged with nitrogen. Spectrophotometric scans from 185 to 385 nm revealed no impurity absorbance bands in the borate. The mineral, chalcocite (from Messina, Transvaal, Republic of South Africa), was prepared under nitrogen by dry grinding with a mortar and pestle and sized from 590 to 840 μm. The particle beds were nominally 1.4 g with a specific surface are [6] of 58 $cm^2 g^{-1}$. Reagent-grade potassium ethylxanthate was recrystallized three times from acetone and ether and refrigerated under nitrogen until used. Stock xanthate solutions were prepared daily in nitrogen-purged borate to ensure minimum decomposition.

Upon introduction of chalcocite to the cell, the mineral bed was electrochemically preconditioned at selected potentials between -0.5 and -0.1 V until the cathodic background current decayed to a steady-state value of 4 to 8 μA. The potassium ethylxanthate was injected into the flow system at a position just before the pump to maximize solution mixing prior to collector contact with the bed. Following injection, the electrochemical current and the xanthate concentration were monitored continuously. The xanthate concentration was determined using the spectral absorbance at 301 nm and the

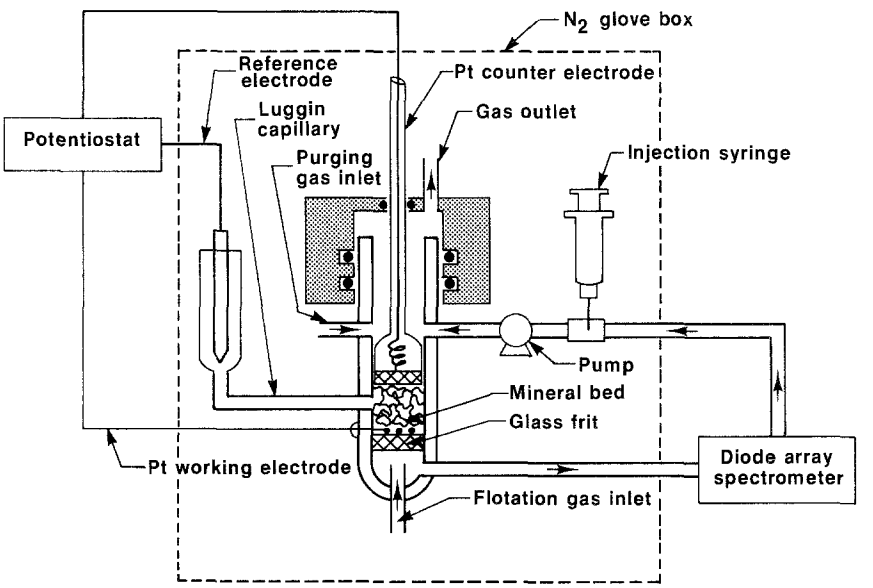

Fig. 1. Electrochemical–microflotation cell and associated equipment.

* Reference to specific products does not imply endorsement by the Bureau of Mines.

volume of the solution in the entire flow system (33 to 35 cm^3).

Dissolved oxygen probe (Lazar Research Labs) measurements indicated oxygen levels of $\sim 80\,\mu g\,l^{-1}$ for the borate solution, which translates to a theoretical limiting diffusion current, i_d, of $\sim 16\,\mu A$ for the mineral bed using

$$i_d = nFADC_0/\delta \quad (4)$$

assuming a four-electron (n) reduction process and for $A = 58\,cm^2$, $D = 1.58\,cm^2\,s^{-1}$ [8], $C_0 = 2.5 \times 10^{-6}$ M oxygen, F is the Faraday constant and $\delta = \sim 0.05$ cm. Since the measured steady-state background current (4 to 8 μA) was of the same magnitude as the theoretical limiting current ($\sim 16\,\mu A$), the major portion of the bed background current can be attributed to oxygen reduction. In comparison, background currents on beds outside the nitrogen dry box [6] were typically 40 to 60 μA (a factor of 10 higher than in the present study).

An additional source of cathodic background current could have resulted from the diffusion of oxygen generated at the counter electrode to the particle bed electrode. However, this diffusion was limited by the use of a fine glass frit (pore size, 4–5.5 μm) which separated the counter electrode from the mineral electrode.

3. Results

3.1. *Background voltammetry*

Cyclic voltammograms of chalcocite bed electrodes in quiescent and flowing solutions (Fig. 2) exhibited well-defined features similar to previously published voltammograms [6, 9] on single-particle electrodes. Electrochemical and spectrophotometric studies of the reactions have been discussed in detail in a previous paper [7], and the results relevant to the present study may be summarized as follows:

1. On anodic sweeps, an oxidation wave commenced at -0.1 V, with at least a part of the current producing a Cu(II) species in the solution phase,
2. During the return cathodic sweep, Cu(II) was reduced, presumably reforming the copper sulphide with a peak at $\simeq -0.1$ V,
3. Cathodic sweeps to more negative potentials gave a reduction wave commencing at $\simeq -0.58$ V with a soluble reduction product of HS^-, and
4. During the return anodic sweep, HS^- reacted, presumably to reform a copper sulphide with a peak at $\simeq -0.6$ V.

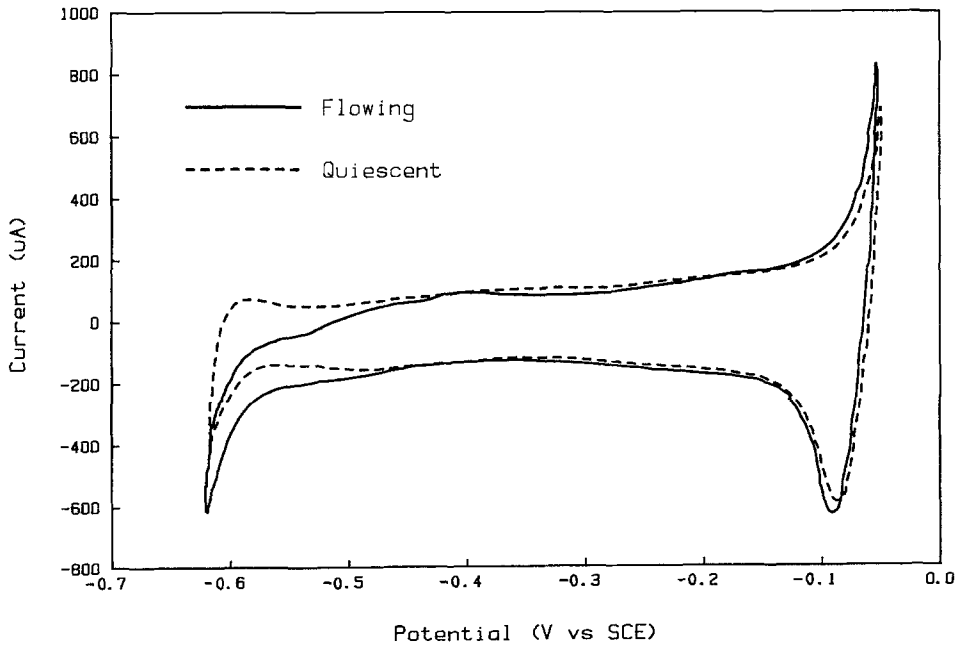

Fig. 2. Cyclic voltammograms of a chalcocite mineral bed in 0.05 M sodium borate. Potential sweep from -0.05 to -0.62 V versus SCE at 10 mV s^{-1}.

Although voltammograms on bed electrodes exhibit the same characteristic reactions at the same potential as those on massive single electrodes, the current density (normalized to the geometric area) is less by a factor of 10 to 20 than that on massive electrodes. It is not believed that this can be accounted for entirely by assuming polished (600 grit) massive electrodes have a surface area 10 to 20 times greater than fractured particles. On the contrary, it has usually been concluded from adsorption studies that polished sulphide electrodes have a true surface area of only 2 to 4 times the geometric area [10, 11]. The large discrepancy in current densities must then be accounted for by assuming either that polished electrodes are much more reactive than fractured particle electrodes or that a non-uniform distribution of potential exists within a bed electrode such that a large fraction of the bed remains unpolarized. In a separate study [12] carried out on 200–300 g bed electrodes in a cell with cylindrical geometry, the local solution and particle potentials were determined using miniature Ag/AgCl and chalcocite electrodes respectively. It was found that the potential drop within the bed occurred primarily in the solution phase, whereas the potential of the dispersed particle phase was nearly constant (independent of position) and was fixed by the dissolved oxygen level. The local potential difference between a particle and the surrounding solution thus varied with position. However, at low oxygen concentrations, such as in the present experiments, this difference was a maximum of $\sim 10\,\mathrm{mV\,cm^{-1}}$. For ordinary Tafel slopes, a spread of potential differences of this magnitude could not account entirely for the reduced activity of the bed electrodes compared to massive electrodes. It is thus likely that a combination of greater reactivity and greater true surface induced by polishing increases the current density of polished massive electrodes, whereas a slight non-uniform potential decreases the apparent reactivity of a fractured particle bed.

Further indications of the narrow range of potential variation within a bed electrode was provided by the flotation recovery induced by an electroactive organic collector [12]. The recovery varies from 0 to 100% over a potential range of $\simeq 100\,\mathrm{mV}$, i.e. the coverage changes from essentially 0 to $\simeq 1$ monolayer on all particles with a variation of only 100 mV in potential.

It is important to note that the working potential of chalcocite electrodes for studying xanthate adsorption was essentially limited to values between -0.6 and $-0.1\,\mathrm{V}$. At more positive potentials, soluble Cu(II) ions from the anodic dissolution of chalcocite reacted with xanthate [6]. In deoxygenated solution, the dominant copper complex at pH 9.2 is $Cu(OH)^+$ when the free Cu^{2+} concentration is $< 2.5 \times 10^{-7}\,\mathrm{M}$ and is $Cu_2(OH)_2^{2+}$ when the free Cu^{2+} concentration is $> 2.5 \times 10^{-7}\,\mathrm{M}$ [13]. The lower limit of $\simeq -0.6\,\mathrm{V}$ prevented the introduction of HS^- into solution by chalcocite reduction with associated changes in the mineral surface, such as cathodic formation of elemental copper [7]. Interactions between xanthate and a copper electrode occur at potentials anodic to $-0.65\,\mathrm{V}$ [11]. While the presence of elemental copper in chalcocite cannot be ruled out completely [14], formation of copper, i.e. forcing the electrode potential cathodic of $-0.6\,\mathrm{V}$, is not a prerequisite for the xanthate–chalcocite processes addressed in this work.

3.2. *Chalcocite–ethylxanthate voltammetry*

Voltammograms of chalcocite-bed electrodes in the presence of ethylxanthate over the range of -0.6 to $-0.1\,\mathrm{V}$ were characterized by three distinct oxidation processes labelled A_1, A_2 and A_3 in Figs 3 and 4. A_1 and A_2 are characteristic of chemisorption processes, and A_3 is characteristic of a diffusion-controlled bulk product reaction; that is, the combined charge of A_1 and A_2 was independent of (1) sweep rate at values less than $5\,\mathrm{mV\,s^{-1}}$, (2) the presence or absence of electrolyte flow, and (3) xanthate concentration at values greater than $2 \times 10^{-5}\,\mathrm{M}$. The diffusion-controlled current due to process A_3 decreased greatly with decreasing sweeps in a quiescent electrolyte (Fig. 4), and in a flowing electrolyte, reached a limiting plateau proportional to xanthate concentration. When the anodic limit was restricted to values in the potential region between A_2 and A_3, two reduction peaks C_1 and C_2 were observed on the return cathodic sweep (Fig. 5), and the charge passed in C_1 and C_2 was equal to the anodic charge of A_1 and A_2. With

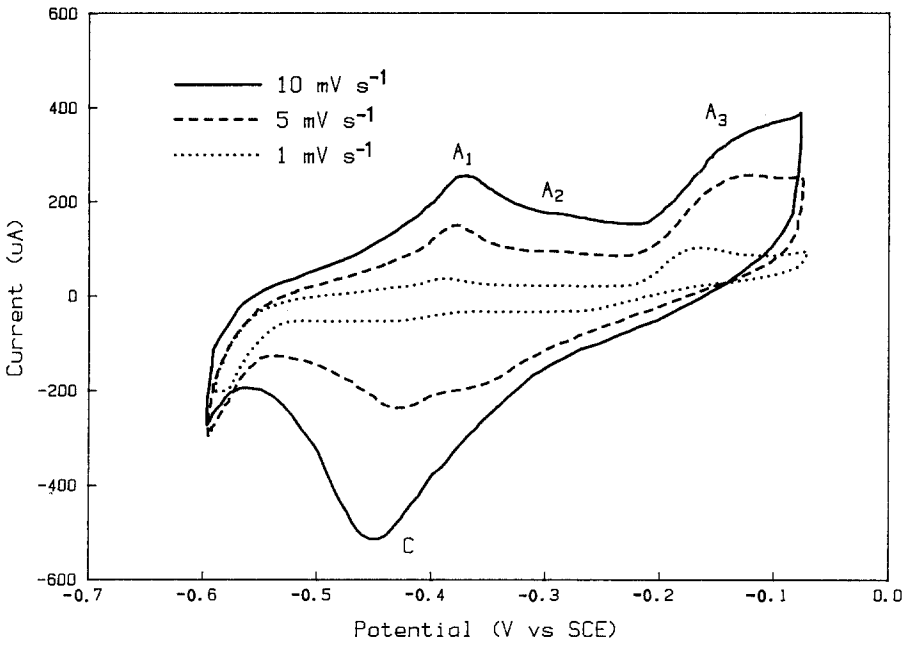

Fig. 3. Cyclic voltammograms of a chalcocite mineral bed in 0.05 M sodium borate with 1.9×10^{-5} M potassium ethylxanthate under flowing conditions. Potential sweep from -0.05 to -0.6 V versus SCE.

increasing anodic limits, peak C (Fig. 3) grew and obscured C_1 and C_2, as shown in Fig. 3.

The above characteristics of an ethylxanthate–chalcocite particle-bed system at pH 9.2 are essentially the same as that found by Kowal and Pomianowski [9] for single-particle electrodes in unbuffered 0.1 M NaF solutions. We have shown in a previous paper [6] that the flotation of chalcocite between the same potential limits as in the present study increases from

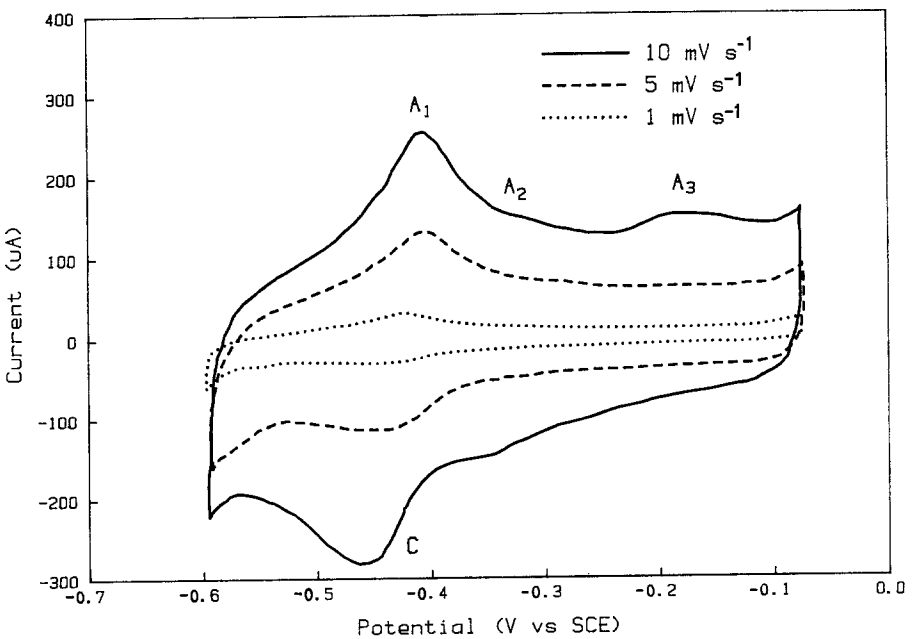

Fig. 4. Cyclic voltammograms of a chalcocite mineral bed in 0.05 M sodium borate with 1.9×10^{-5} M potassium ethylxanthate under quiescent conditions. Potential sweep from -0.05 to -0.6 V versus SCE.

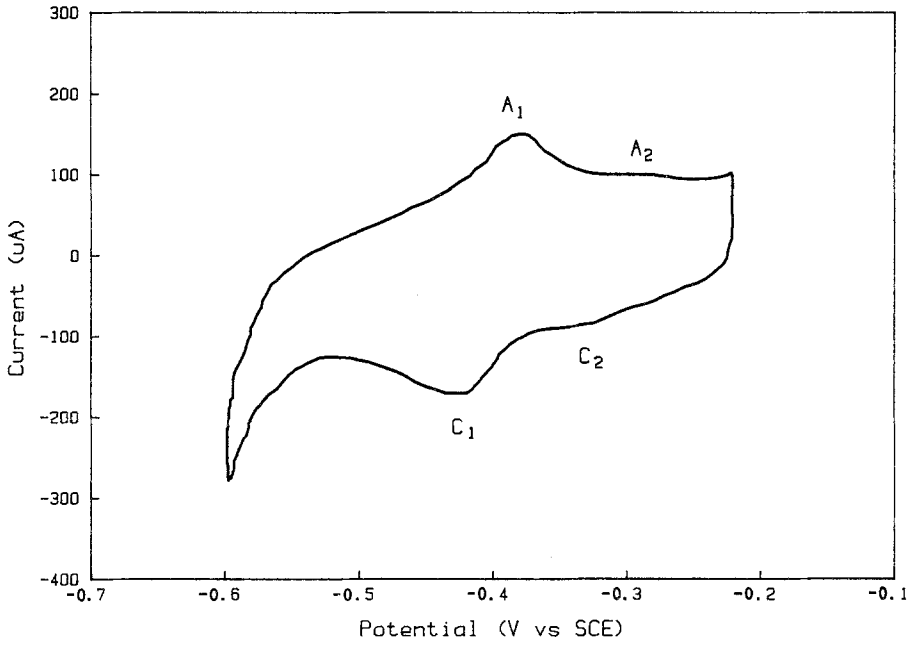

Fig. 5. Cyclic voltammogram of a chalcocite mineral bed in 0.05 M sodium borate with 1.9×10^{-5} M potassium ethylxanthate under flowing conditions. Potential sweep from -0.23 to -0.6 V versus SCE at 5 mV s^{-1}.

0% at -0.6 to $\geqslant 90\%$ at -0.3 V; therefore, it can be concluded that the chemisorption reactions associated with A_1 and A_2 are sufficient for flotation.

3.3. *Chalcocite–ethylxanthate reactions under potentiostatic conditions*

The effect of preconditioning potential on the

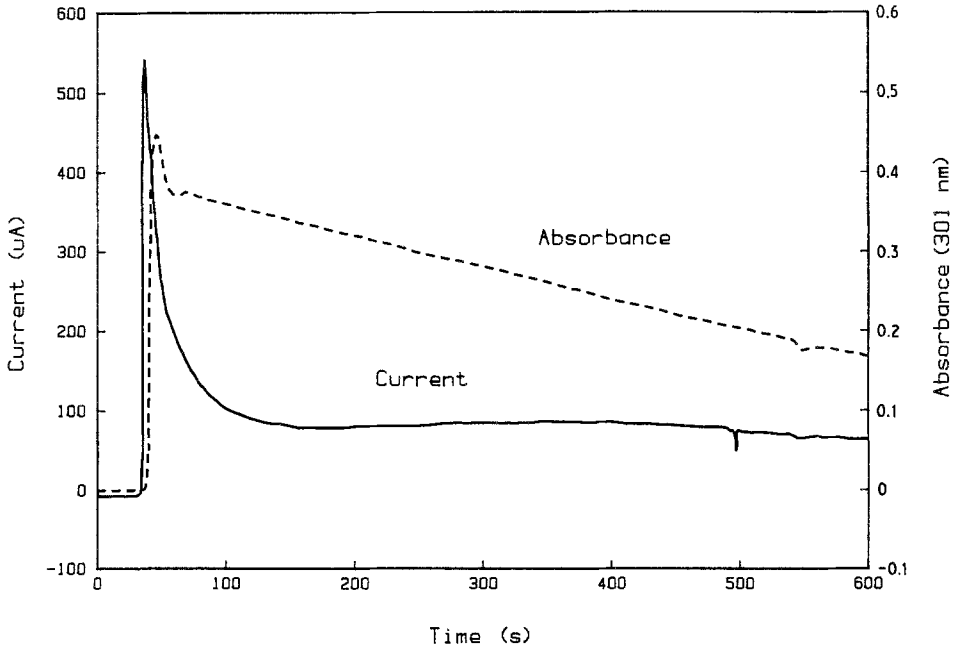

Fig. 6. Current and absorbance changes for the chalcocite system at -0.15 V versus SCE following injection of 2×10^{-5} M potassium ethylxanthate.

extent of the electrochemical interaction between xanthate and chalcocite was determined by potentiostating fresh beds at various potentials between -0.6 and -0.1 V and injecting xanthate into the system. Prior to injection, the solutions were thoroughly purged with nitrogen until the current reached a small steady-state value, indicating that residual oxygen had reached its lowest value.

Fig. 6 shows typical plots of the electrolysis current and absorbance at 301 nm associated with the injection of xanthate. The time delay in absorbance response relative to the current response was $\simeq 2$ s and represented the time required for the xanthate solution to flow from the bed to the UV cuvette. Oscillations in absorbance prevented quantitative measurement of the changes in xanthate concentration during the 30 s required to achieve homogeneous mixing.

The change with time, t, in xanthate concentration $[\Delta X(t)]_{EC}$ produced by a charge-transfer oxidation reaction can be compared with the total change in xanthate $[\Delta X^-]_T$ through Beer's law and Faraday's second law:

$$[\Delta X^-]_T = \Delta A_{301}(t)/L\varepsilon_{301} \quad (5)$$

$$[\Delta X^-]_{EC} = \Delta Q(t)/nFV \quad (6)$$

where L is the light pathlength, ε_{301} and ΔA_{301} are the molar absorptivity, 17 750 $l\,cm^{-1}\,mol^{-1}$ [15], and change in absorbance of ethylxanthate at 301 nm, respectively, $Q(t)$ is the electrolysis charge, n the number of electrons, F is the Faraday constant and V is the solution volume in litres. If we assume that changes in xanthate concentration may also have non-electrochemical components, $[\Delta X^-]_{NEC}$, the total change in xanthate concentration can be written

$$[\Delta X^-]_T = [\Delta X^-]_{EC} + [\Delta X^-]_{NEC} \quad (7)$$

or by combining Equations 5 and 6

$$\Delta A_{301}/L\varepsilon_{301} = \Delta Q/nFV + [\Delta X^-]_{NEC} \quad (8)$$

Assigning $n = 1$ and plotting $[\Delta X^-]_T$ from the UV spectral data versus $[\Delta X^-]_{EC}$ from Equation 8 should yield a straight line, with a slope of unity, which passes through the origin if the reaction were totally electrochemical.

Figs 7 and 8 are experimental plots of $\Delta A_{301}/L\varepsilon_{301}$ versus Q/FV for beds potentiostated at various potentials between -0.5 and -0.1 V. The dashed line through the origin is the behaviour expected from Equation 8 for a one-electron oxidation reaction ($n = 1$) with no

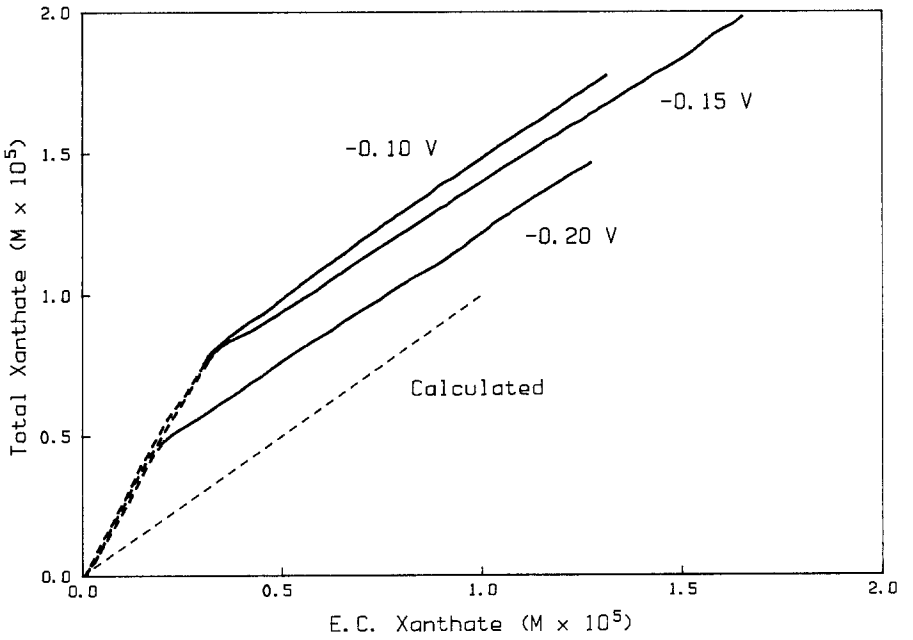

Fig. 7. Ethylxanthate adsorbed measured spectrophotometrically plotted against the xanthate consumed electrochemically for potentials of -0.10, -0.15, and -0.20 V versus SCE. Dashed line calculated for a 100% electrochemical process.

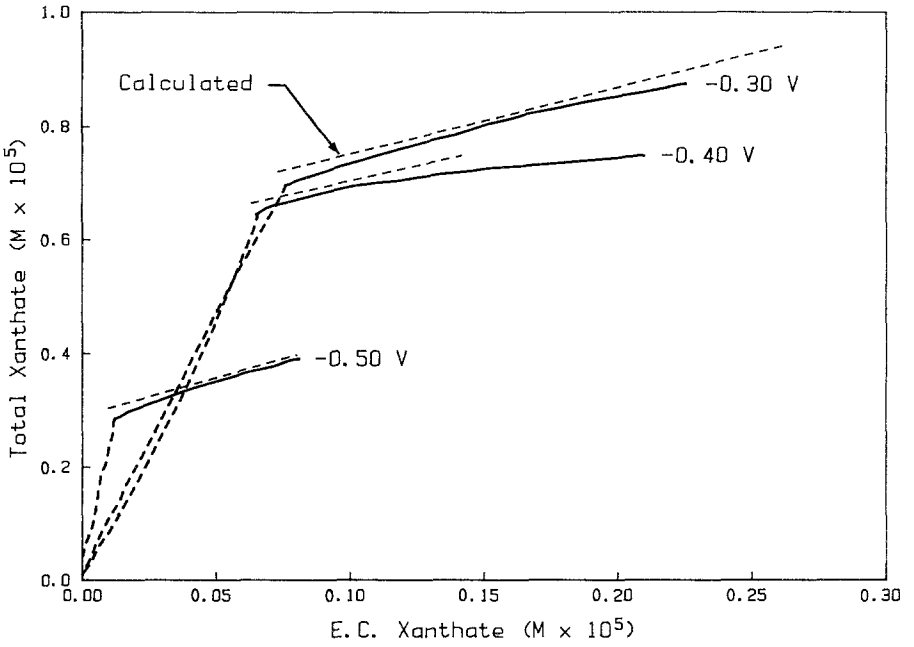

Fig. 8. Ethylxanthate adsorbed measured spectrophotometrically plotted against the xanthate consumed electrochemically for potentials of −0.30, −0.40, and −0.50 V versus SCE. Dashed lines calculated for a one-electron electrochemical process.

other reactions of xanthate ($[\Delta X^-]_{NEC} = 0$). (Slopes greater than unity imply a non-electrochemical consumption of xanthate, $[\Delta X^-]_{NEC} < 0$; for example, exchange reactions, adsorption on the walls of the apparatus or xanthate decomposition. Regions with a slope less than unity imply non-electrochemical production of xanthate, $[\Delta X^-]_{NEC} > 0$.) The slopes of the solid curves of Fig. 7 vary slightly, but the minimum and maximum slopes observed were 0.847 and 0.952, respectively. These values are within the experimental uncertainty in ε_{301} and the volume measurements. The slopes are equivalent to $n = 1.38$ and 1.05, establishing that the reaction is predominately a one-electron oxidation process except at very short times. The curvature is believed to represent a small contribution by a chemical process, possibly due to decomposition of ethylxanthate. With the exception of the curve for −0.4 V, the $\Delta A/L\varepsilon_{301}$ versus $\Delta Q/FV$, plots of Fig. 8 are also close to unity slope at long reaction times.

An interesting feature of the data is that, although the curves have a slope near unity as expected for a one-electron oxidation reaction, they do not pass through the origin, implying that a rapid non-electrochemical decrease in xanthate occurred during or shortly after xanthate injection. It should be noted that the slight displacement between the absorbance and current curves (Fig. 6), resulting from the time for the solution to flow from the bed to the cuvette, has a negligible effect on the slope at long times and on the extrapolated intercept. Moreover, adsorption onto the system walls or any reactions of ethylxanthate with Cu(II) released from the beds either as soluble Cu(II) complexes or as precipitates apparently cannot account for the rapid initial decrease in xanthate concentration. After potentiostating at −0.3 V for 45 min, the solution and mineral bed were removed from the cell and the cell gently washed and refilled with borate. Titration of the original solution and of the refilled cell established that reactions involving xanthate were negligible, i.e. consumed $\leqslant 10^{-7}$ M. Thus, the non-electrochemical reaction appeared to take place on the mineral bed, probably in an ion exchange process such as that represented by Reaction 2a. The non-electrochemical process removed between 15 and 25% (3 to 5 × 10^{-6} M) of the xanthate from the solution phase within the first 30 s; thereafter, the charge-transfer process became the dominant reaction.

4. Discussion

From cyclic voltammetry, two oxidation reactions have been identified between -0.5 and -0.1 V for the chalcocite–xanthate system at pH 9.2. A chemisorption reaction occurred between $\simeq -0.5$ and -0.3 V; above -0.23 V, the formation of a bulk oxidation product occurred. Cuprous xanthate is the likely bulk oxidation product from thermodynamic considerations [16–18] and from solvent extraction studies [19, 20]. For chalcocite exposed to xanthate concentrations at and below monolayer coverage requirements, the adsorbed layer was reported to be unleachable with most solvents; however, pyridine was found to extract cuprous xanthate and the leachable film was sufficient to produce flotation [19]. The potential at which the onset of xanthate chemisorption occurred was $\simeq -0.5$ V (Fig. 3), which, as discussed by Heyes and Trahar [17] and Richardson *et al.* [6], is significantly more negative than the reversible thermodynamic potentials expected for reactions between chalcocite and xanthate to form cuprous or cupric xanthate. Thus, the reactions between $\simeq -0.5$ and -0.3 V appear to represent underpotential deposition of xanthate on chalcocite.

Under potentiostatic conditions, injection of xanthate into the system produced a current transient and a change in xanthate concentration. Two distinct xanthate consumption mechanisms have been identified. First, a fast non-electrochemical reaction occurred consuming 15 to 25% of the added xanthate. This is believed to occur by an ion-exchange process. Second, at times $\geqslant 30$ s, the reaction of Cu_2S with xanthate is predominately electrochemical, through a chemisorption mechanism at potentials between -0.5 and -0.3 V and a diffusion-controlled process at potentials $\geqslant -0.23$ V.

It is significant that the ethylxanthate concentration used in the present work is close to the concentration used in industrial flotation circuits. Thus, the reactions identified electrochemically can be directly compared with flotation response without correcting for concentration effects. In this regard, Heyes and Trahar [17], using reducing and oxidizing reagents, and Richardson *et al.* [6], using a direct electrochemical method, have established that the flotation edge of chalcocite occurs at

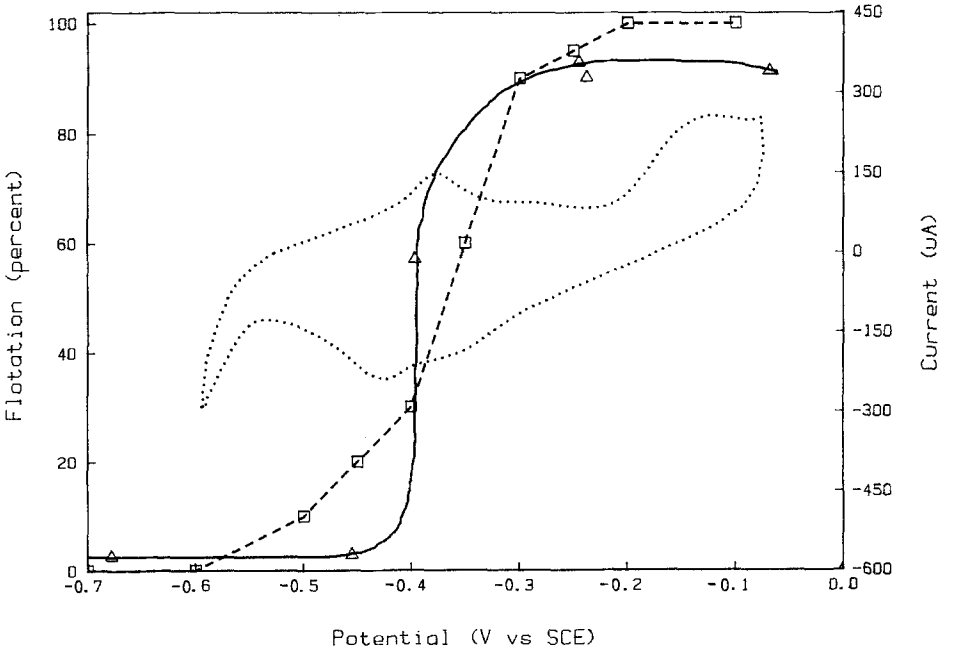

Fig. 9. Comparison of the flotation response and voltammogram of chalcocite using ethylxanthate as the collector showing correlation between flotation and xanthate chemisorption represented by A_1. The xanthate concentrations for Heyes and Trahar [17] (——), Richardson *et al.* [6] (– – –), and the present work (···) were 4.7×10^{-5} M, 1.44×10^{-5} M, and 1.9×10^{-5} M, respectively.

$\simeq -0.4$ V. Their results are shown in Fig. 9; the excellent correlation between the flotation edge and xanthate chemisorption is obvious. It has also been determined that when Cu_2S is rendered floatable at oxidizing potentials, it can be subsequently depressed at reducing potentials [6, 17]. The excellent correlation of the flotation edge with the xanthate chemisorption peak observed on voltammograms, as well as the depression at reducing potentials, provide convincing evidence that the reaction that renders Cu_2S floatable is electrochemical in origin.

From the present experiments, no plausible explanation is available for the role, if any, of the fast non-electrochemical component of the reactions. This component, with the exception of the data at -0.5 V, appears to be nearly independent of potential and causes a xanthate concentration decrease of $\simeq 5 \times 10^{-6}$ M. The non-electrochemical component may be a function of surface oxidation [21, 22] with ion exchange between xanthate and the surface hydroxides. If ion exchange, such as Reaction 2a, is the operative mechanism, then the pH should change in unbuffered solutions. As example, for the particle-bed size and surface areas used in this work and assuming an adsorbed ethylxanthate molecule occupies an area of 0.28 nm^2 [23], 4.8×10^{-8} mol of xanthate would provide monomolecular bed coverage. For a solution volume of 35 cm^3, the corresponding change in xanthate concentration should be 1.4×10^{-6} M, slightly smaller than the xanthate consumed by the fast non-electrochemical component ($\simeq 5 \times 10^{-6}$ M). A xanthate: hydroxide ratio of 1 : 1 during an ion exchange reaction should, therefore, increase the hydroxide concentration by 1.4×10^{-6} M. In an initial unbuffered solution of pH 9.00, the total hydroxide thus becomes 1.14×10^{-5} M, equivalent to pH 9.06. Using an unbuffered solution (pH 9.00 sodium hydroxide) in our chalcocite system, no pH change was detected upon addition of 2×10^{-5} M ethylxanthate. The pH was monitored with a Ross-type electrode that detects changes of < 0.002 pH unit. Although a rise in pH has been reported [22], we have not seen a change in our system. From previous studies [6], this non-electrochemical process should have been sufficient to induce chalcocite flotation if the product were hydrophobic and adsorbed on the surface, i.e. if it were formed by an ion-exchange process. However, the decrease in xanthate by the non-electrochemical process was, at most, only weakly dependent on potential, inconsistent with the strong dependence of flotation on potential.

5. Conclusions

Cyclic voltammetry on particle-bed chalcocite electrodes yielded well-defined features similar to those reported on single-particle electrodes. These reactions were characteristic of chemisorption commencing at -0.5 V followed by the formation of a diffusion-controlled oxidation product above -0.23 V.

Relating the charge passed on a chalcocite mineral bed after addition of xanthate to spectrophotometric change in xanthate concentration established the occurrence of two types of reaction. A fast chemical reaction occurred, consuming ~ 15 to 25% of the xanthate. This reaction seemed to have no effect on flotation since the xanthate consumed by this process remained nearly constant as the potential was varied, whereas the flotation response was potential dependent. After ~ 30 s, the reactions involving xanthate became primarily a one-electron charge-transfer processes. Correlation between the flotation and electrochemical data provides ample evidence that the chemisorption of xanthate ($\geqslant -0.5$ V) produces a hydrophobic surface capable of inducing flotation. At potentials $\geqslant -0.23$ V, the hydrophobicity necessary for flotation was maintained during the production of a bulk copper xanthate.

Acknowledgement

This paper was originally presented at the spring 1984 meeting of The Electrochemical Society, Inc., held in Cincinnati, Ohio. The authors acknowledge the permission of the Society to publish here.

References

[1] S. G. Salamy and J. C. Nixon, 'Recent Developments in Mineral Dressing,' Institution of Mining and Metallurgy, London (1953) pp. 503–16.

[2] R. Woods, *J. Phys. Chem.* **75** (1971) 354.
[3] I. N. Plaksin and R. Sh. Shafeev, *Bull. Inst. Min. Metal.* **72** (1963) 715.
[4] J. R. Gardner and R. Woods, *Aust. J. Chem.* **26** (1973) 1635.
[5] S. Chander and D. W. Fuerstenau, *Int. J. Miner. Process.* **10** (1983) 89.
[6] P. E. Richardson, J. V. Stout III, C. L. Proctor and G. W. Walker, *ibid.* **12** (1984) 73.
[7] G. W. Walker, J. V. Stout III and P. E. Richardson, *ibid.* **12** (1984) 55.
[8] B. Miller and J. M. Rosamilia, *Anal. Chem.* **56** (1974) 2410.
[9] A. Kowal and A. Pomianowski, *J. Electroanal. Chem.* **46** (1973) 411.
[10] T. Biegler and M. D. Horne, 'Proceedings of the International Symposium on Electrochemistry in Mineral and Metal Processing', edited by P. E. Richardson, S. Srinivasan and R. Woods, The Electrochemical Society Inc., Pennington, New Jersey (1984) p. 321.
[11] R. Woods, *J. Phys. Chem.* **75** (1971) 354.
[12] J. E. Gebhardt, N. F. Dewsnap and P. E. Richardson, Bureau of Mines RI 8293, United States Department of the Interior (1985).
[13] Y. A. Attia, *Trans. Inst. Min. Metall.* **85** (1975) C221.
[14] R. W. Potter II, *Econ. Geol.* **72** (1977) 1524.
[15] A. Pomianowski and J. Leja, *Can. J. Chem.* **41** (1963) 2219.
[16] T. Hepel and A. Pomianowski, *Int. J. Miner. Process.* **4** (1977) 345.
[17] G. W. Heyes and W. J. Trahar, *ibid.* **6** (1979) 229.
[18] W. J. Trahar, 'Principles of Mineral Flotation: The Wark Symposium' (edited by M. H. Jones and J. T. Woodcock), The Australasian Institute of Mining and Metallurgy, Victoria, Australia (1984) p. 117.
[19] A. M. Gaudin and R. Schuhmann Jr, *J. Phys. Chem.* **40** (1936) 257.
[20] P. J. Harris and N. P. Finkelstein, Report No. 1896, National Institute for Metallurgy, Randburg, South Africa (1977).
[21] W. Barzyk, K. Malysa and A. Pomianowski, *Int. J. Miner. Process.* **8** (1981) 17.
[22] Z. Adamczyk, W. Barzyk, J. Czarnecki and A. Pomianowski, *ibid.* **7** (1980) 57.
[23] V. I. Klassen and V. A. Mokrousov, 'An Introduction to the Theory of Flotation', Butterworth, London (1963) p. 237.